The Rational Design of Highly Potent and Selective Covalent MAP2K7 Inhibitors

Dalton R. Kim,[1] Meghan J. Orr,[1] Ada J. Kwong,[1] Kristine K. Deibler,[1] Hasan H. Munshi,[1] Cory Seth Bridges,[2] Taylor Jie Chen,[2] Xiaoyu Zhang,[1,3] H. Daniel Lacorazza,[2] and Karl A. Scheidt[1,3,4]*

[1]Department of Chemistry, Northwestern University, Evanston, Illinois 60208, United States.

[2]Department of Pathology & Immunology, Baylor College of Medicine, Houston, Texas 77030, United States.

[3]Chemistry of Life Processes Institute, Northwestern University, Evanston, Illinois 60208, United States.

[4]Department of Pharmacology, Feinberg School of Medicine, Northwestern University, Chicago, Illinois 60611, United States.

ABSTRACT: The mitogen-activated protein kinase signaling cascade is conserved across eukaryotes from yeast to humans, where it plays a central role regulating activities including proliferation, differentiation, and stress responses. This pathway propagates external stimuli through a series of phosphorylation events, allowing external signals to influence metabolic and transcriptional activities. Within the cascade, MEK, or MAP2K, enzymes occupy a molecular crossroads situated immediately upstream to significant signal divergence and cross-talk. One such kinase, MAP2K7, also known as MEK7 and MKK7, is a protein of great interest in the molecular pathophysiology underlying pediatric T-cell acute lymphoblastic leukemia. Herein, we describe the rational design, synthesis, evaluation, and optimization of a novel class of irreversible MAP2K7 inhibitors. With a streamlined one-pot synthesis, favorable *in vitro* potency and selectivity, as well as promising cellular activity, this novel class of compounds wields promise as a powerful tool in the study of pediatric T-ALL.

Acute lymphoblastic leukemia (ALL) is a deadly blood cancer and the most common hematological malignancy in pediatric patients under 14 years of age. Roughly 6,000 cases of ALL are diagnosed annually in the United States,[1] with half of these cases occurring in children and adolescents.[2] Despite advancements in treatments and improvement in outcomes,[3] ALL remains the most frequent cause of death from cancer before the age of 20,[4] and relapse continues to be the leading cause of cancer-related mortality in children.[5] Nearly a quarter of pediatric patients and over half of adult patients with T-cell ALL (T-ALL) exhibit resistance to therapy and ultimately relapse.[3b] Further, survivors of childhood ALL are at risk for a multitude of sequelae due to multi-agent chemotherapy,[6] which has evolved only incrementally since the first descriptions of "total therapy" of T-ALL by Donald Pinkel.[7] Targeted therapies for children with high-risk T-ALL have been an area of active research.[8]

Krüppel-like factor 4 (KLF4) is a zinc-finger transcription factor[9] known to function as either an oncogene or a tumor suppressor in a context-dependent manner.[10] Epigenetic silencing of *Klf4* by CpG methylation is known to occur in pediatric ALL, and decreased KLF4 expression has been identified in treatment-resistant cases of ALL.[11] Physiologically, KLF4 represses transcription of *Map2k7,* a gene encoding mitogen-activated protein kinase kinase 7 (MAP2K7), also known as MAPK/Erk kinase 7 (MEK7, or MKK7).[8b] Loss of *Map2k7* repression and consequent amplification of downstream mitogen-activated protein kinase (MAPK) signaling is thought to contribute to T-ALL pathology.[8b,12] Inhibition of MEK7[13] or its substrate *c*-Jun *N*-terminal kinase (JNK)[8b] has been shown to reduce leukemic expansion in patient-derived xenograft mouse models.

Given that JNK is the only known substrate of MAP2K7,[8b,14] selective inhibitors of JNK are logical chemical probes for the study of MAPK dysregulation in T-ALL. However, JNK is also implicated in genomic stability through its roles in the repair of DNA double-strand breaks[15] and photodamage,[16] but these activities are not known to be MAP2K7-dependent. Therefore, direct inhibition of MAP2K7 would facilitate a more valid investigation of *Klf4* inactivation and the consequences of the resultant amplification of MAPK pathway signaling in T-ALL.

Recent efforts towards the development of novel MAP2K7 inhibitors have been the subject of a review.[17] The fungal natural product 5Z-7-oxozeaenol (5Z7O, **1**) was found to covalently engage MAP2K7 at Cys218 as determined by X-ray crystallography (Figure 1B).[18] Inhibition of MAP2K7 by 5Z7O was found to induce apoptosis in T-ALL in a dose-dependent manner.[13a] However, 5Z7O potently inhibits a variety of other kinases, including MAP kinase kinase kinase (MAP3K) TAK1.[19] Furthermore, despite covalent engagement, **1** boasts only moderate potency against MEK7 (IC$_{50}$ = 1.3 μM).[18] In 2019, a high-throughput *in silico* screen of over 100,000 acrylamide compounds identified the first series of potent and selective MAP2K7 inhibitors (**2a-d**), reported by London and coworkers.[20] The covalent engagement of these indazole-based arylacylamides with MAP2K7 was confirmed by X-ray crystallography and mass spectrometry. An additional class of covalent MAP2K7 inhibitors based on the pyrazolopyrimidine scaffold has also been disclosed (**3a,b**),[21] the design of which leveraged similarities between the MAP2K7 and EGFR binding pockets. Finally, a series of dual MAP2K4/MAP2K7 inhibitors were reported in 2020 by Gray and Zhang.[22]
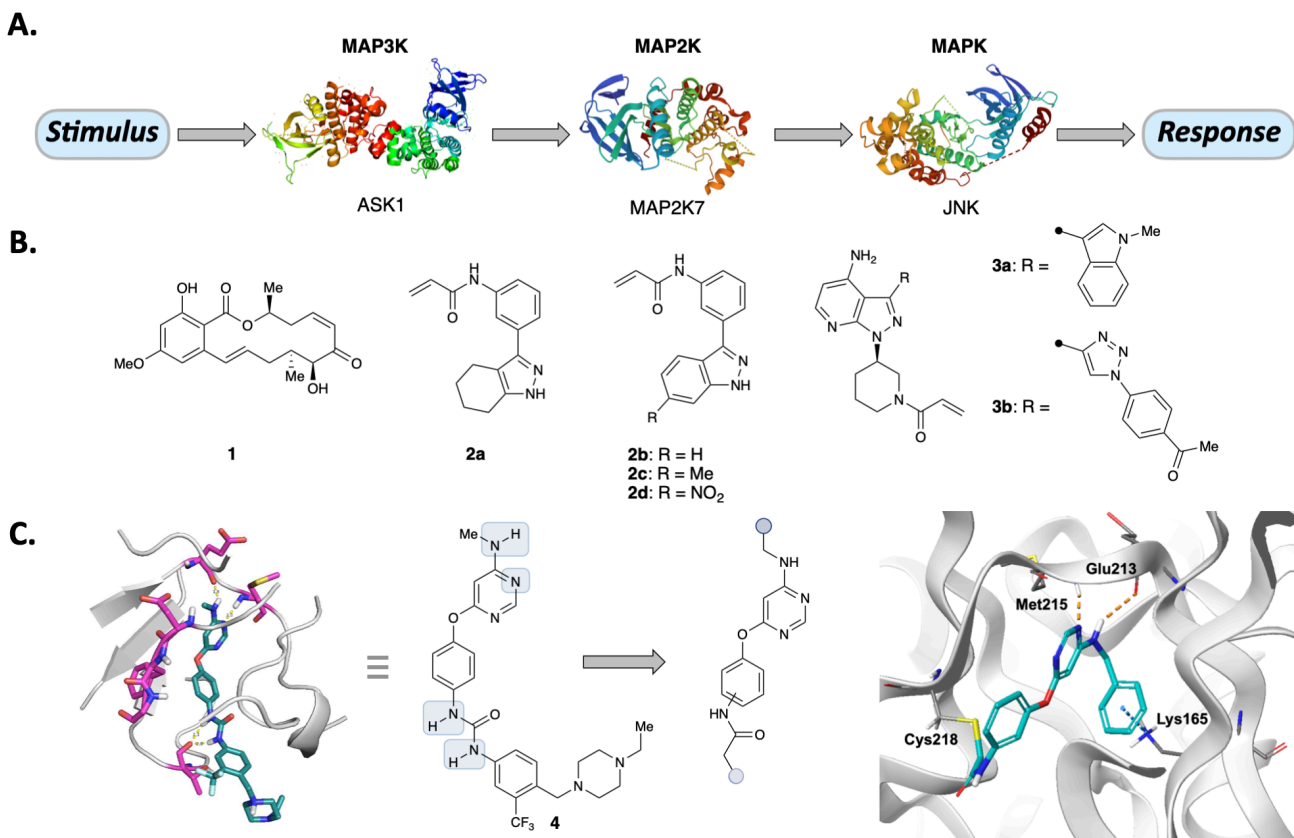
Figure 1. (A) Simplified MAPK signaling cascade. (B) Structures of known MAP2K7 inhibitors. (C) This work constitutes a structure-based approach towards the optimization of AST-487 as a MAP2K7 inhibitor. Enabling a key cation-π interaction and employing an electrophilic moiety endowed the optimized compound with markedly higher potency and selectivity.

We previously reported a chemical probe strategy for interrogating inhibitor selectivity across all seven MEK isoforms.[23] Therein, we describe a functional *in vitro* profiling platform utilizing the ADP-Glo kinase assay[24] and demonstrated its validity against commercially-available kinase inhibitors with known off-target binding affinity to MAP2K4. Despite sharing moderate structural homology and a common phosphorylation substrate in JNK, MAP2K4 and MAP2K7 exhibited strikingly dissimilar susceptibility to the selected panel of kinase inhibitors. Notably, only FMS-like-tyrosine kinase 3 (FLT3) inhibitor AST-487 (**4**, Figure 1C)[25] demonstrated sub-micromolar MAP2K7 inhibition; similar AST-487 potency was otherwise seen only against the rather promiscuous MAP2K5 isoform.

Structural analysis of MEK ATP binding pockets identified MAP2K7 to have a characteristically long and shallow cavity, and quantification confirmed it to have the shallowest depth and smallest volume among all MEK isoforms with available crystal structures.[23] MAP2K7 is also unique among the MEK family for the presence of four cysteine residues in its active site.[23] Notably, it is the only MEK isoform featuring a hinge region cysteine (Cys218),[23] and only 11 human kinases bear a cysteine at the same relative position.[26] Consequently, we envisioned the development of a novel irreversible MAP2K7 inhibitor leveraging these combined structural insights (**Figure 1C**).

We commenced with the synthesis of truncated AST-487 derivatives retaining the structural motifs most responsible for its binding. A streamlined synthesis inspired by an established process synthesis[25a] of AST-487 was developed to access synthetic analogues of interest. Each of the proposed compounds was

prepared by a one-pot process which afforded the desired MAP2K7 inhibitor following aqueous workup and silica gel column chromatography (Scheme 1). This high-yielding procedure features excellent convergence and atom economy, enabling the rapid generation of chemical diversity.
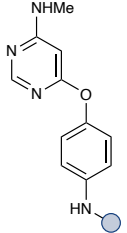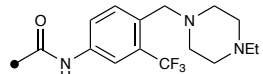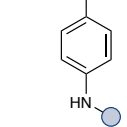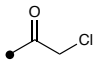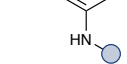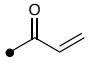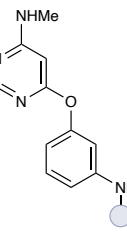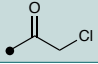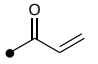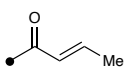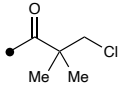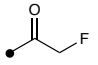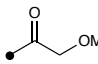
Scheme 1. One-pot process towards the synthesis of novel MAP2K7 inhibitors.
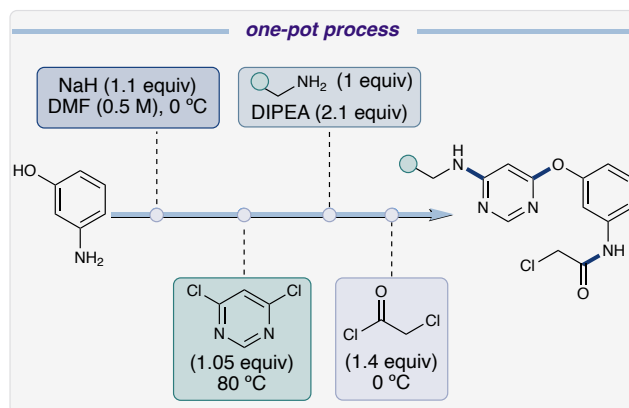
With preliminary derivatives and controls in hand, we commenced their biological characterization by surveying their respective *in vitro* inhibitory capacities towards MAP2K7. Kinase inhibition was determined by a luciferase-based luminescent assay. As shown in Figure 2, **7** demonstrated impressive inhibitory capacity against MAP2K7, (IC$_{50}$ = 60 nM) surpassing that of AST-487 (**4**,

IC$_{50}$ = 260 nM). In contrast, compounds **5**, **6**, and **8** were significantly less active than the lead compound. To probe steric congestion in the proximity of the electrophile, compounds **9** and **10** were prepared and assayed. Surprisingly, neither of these compounds demonstrated measurable activity. This experimental finding is rationalized by computational modeling of **7**, which suggested a great deal of steric congestion in proximity to Cys218 (Figure 2). Exchanging the electrophilic α-chloroacetamide for the less reactive α-fluoroacetamide (**11**) or α-methoxyacetamide (**12**) resulted in greatly attenuated activity, implying a covalent mechanism.

Table 1. *In vitro* potency of preliminary MAP2K7 inhibitors as determined by the ADP-Glo assay.

Structure	Compound	R	IC$_{50}$ (μM)
(structure: NHMe-pyrimidine-O-phenyl-NH)	4	(acetamide-aryl-piperazine-NEt, CF$_3$)	0.26
	5	(COCH$_2$Cl)	1.8
	6	(CO-vinyl)	8.8
	7	(COCH$_2$Cl)	*0.060*
	8	(CO-vinyl)	0.42
(structure: NHMe-pyrimidine-O-phenyl-NH, meta)	9	(CO-CH=CH-Me)	> 80
	10	(CO-C(Me)(Me)-CH$_2$Cl)	> 80
	11	(COCH$_2$F)	7.8
	12	(COCH$_2$OMe)	> 80

Given the greater potency endowed by the α-chloroacetamide electrophilic motif and meta-substitution around the arene, we focused our efforts on compounds of this nature. Although all FDA-approved covalent inhibitors to date feature electrophilic acrylamides or epoxyketones,[27] the half-life of α-chloroacetamides surpasses that of acrylamides in the presence of glutathione at physiological temperature and pH.[28] We hoped to leverage this preliminary structure-activity relationship trend to explore this highly reactive and less frequently employed electrophile[29] that has enjoyed recent success.[30]

We next probed the chemical space with respect to aminopyrimidine functionality. The chloropyrimidine intermediate (**SI-1**) was functionalized with a variety of phenethylamines, other primary amines, as well as secondary amines (**Table 2**). As a whole, compounds with less steric congestion in close proximity to the pyrimidine fared better, with select arylethylamine-derived inhibitors (**14** and **18**) demonstrating the greatest potency. Even moderately sterically-demanding substitution along the appendant arene was associated with lowered potency (*e.g.*, **20-22**).
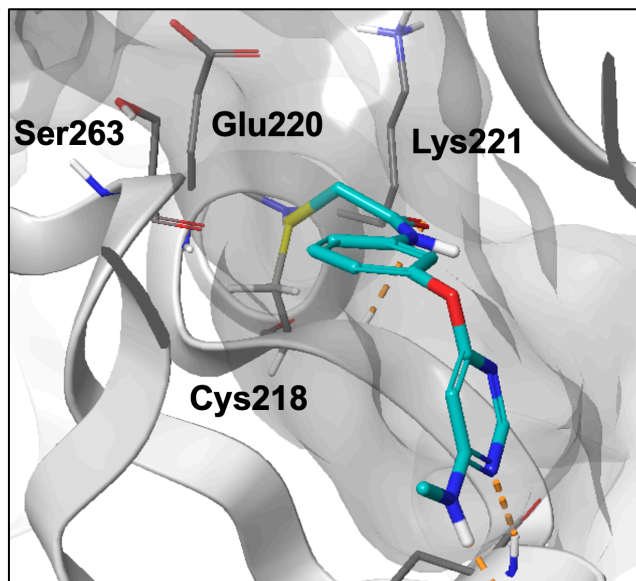
Figure 2. Compound **7** (60 nM) was modeled to bind with its appendant electrophile in close proximity to Cys218. However, apparent steric congestion around the electrophilic center leads to substantially less potent analogues with substitution near the warhead (*e.g.*, **9** and **10**).

These findings were paralleled by docking studies: substituted phenethylamines suffered from steric bulk at the non-electrophilic end of the molecule without gaining additional favorable interactions. This observation is in stark contrast with benzylamine-derived inhibitors, which computational studies predicted to engage in an additional cation-π interaction with Lys165 (Figure 3). This interaction additionally appears to steer the carbon skeleton of the inhibitor away from unfavorable steric interactions.
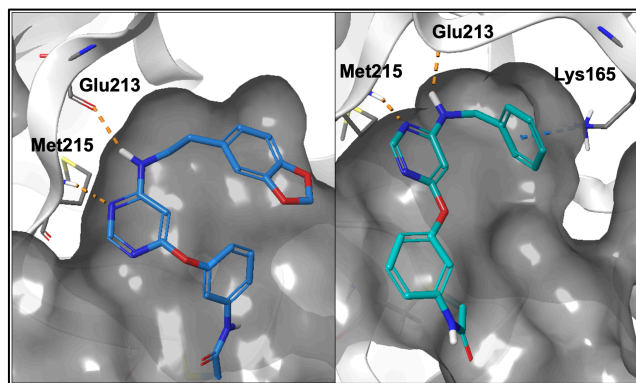
Figure 3: Head-to-head comparison of docking with 3,4-methylenedioxyphenethylamine-derived inhibitor (**22**) and benzylamine-derived inhibitor (**24**). Steric congestion is thought to underlie poor potency of substituted phenethylamine derivatives and better fit of benzylamine analogues.

Guided by these new insights, we next designed, synthesized, and evaluated a new class of benzylamine-functionalized pyrimidines (Table 3). Gratifyingly, the simplest of these compounds, **24** (DK2403), demonstrated extremely high potency (IC$_{50}$ = 10 nM). The potency of its *N*-methylated derivative (**23**) suffered an attenuation of an order of magnitude, highlighting the importance of this key hydrogen bond.

Table 2. *In vitro* potency of MAP2K7 inhibitors with varying pyrimidine substitution as determined by ADP-Glo assay.

Structure	Compound	R	IC$_{50}$ (µM)
	13	morpholine	0.90
	14	indol-3-yl-ethylamine	0.26
	15	cyclopentylamine	0.27
	16	tetrahydropyran-4-ylamine	1.5
	17	R = H	1.2
	18	R = 4-Cl	0.066
	19	R = 4-F	1.2
	20	R = 4-MeO	0.93
	21	R = 3-MeO, 4-MeO	1.7
	22	R = 3,4-O(CH$_2$)O	1.1

Structure	Compound	R	IC$_{50}$ (µM)
	23	Ph-CH$_2$-N(Me)-	0.11
	24	R = H	*0.010*
	25	R = 3-F, 5-F	0.074
	26	R = 2-F, 4-F	0.36
	27	R = 2-F, 3-F, 6-F	0.11
	28	R = 3-F, 4-F	*0.042*
	29	R = 2-CF$_3$	1.2
	30	R = 3-CF$_3$, 4-F	3.0
	31	R = 2-OMe	0.80
	32	R = 3-CF$_3$, 5-CF$_3$	6.3
	33	R = 4-OMe	0.30
	34	R = 3-OMe, 4-OMe	0.26
	35	R = 4-Me	0.36
	36	R = 4-CF$_3$	0.41

Substitution around the arene generally led to a decrease in potency, with some positions and substitutions being tolerated better than others. Small substituents such as fluorine atoms were well tolerated (**25**-**28**), with the 3,4-difluorinated derivative (**28**) demonstrating 42 nM potency. Substituents as large as a methyl group invariably led to decreased potencies, and substitution at the *ortho* position (**29**, **31**) pushed potencies towards the micromolar range. Larger substituents were better tolerated in the *para* (**33**, **35**) and *meta* (**34**) positions, although di-substitution at the *meta* positions was poorly tolerated (**32**).

With a series of highly potent MEK7 inhibitors in hand, we next probed the selectivity of these compounds. Among the MEK isoforms, MEK7 shares the greatest structural homology with MEK4, making it the key kinase to test as we commence selectivity studies.[31] Potency was determined against MEK4 employing our standard protocol (*vide supra*). Much to our surprise, compounds **7**, **8**, and **24** showed virtually no activity against MEK4 (IC$_{50}$ > 80 µM, Figure 4). When studied against the MEK3, 5, and 6 isoforms, **7** and **8** were again found to be inactive (See Figure SI-1).

Table 3. *In vitro* potency of benzylamine-derived MAP2K7 inhibitors as determined by ADP-Glo assay.

substituents	MEK4	MEK7	selectivity ratio
Me (7)	> 80 µM	60 nM	> 1300
Me (8)	> 80 µM	260 nM	> 310
Ph (24)	> 80 µM	10 nM	> 8000

Figure 4: MEK7/MEK4 selectivity profiles of select inhibitors

MEK4 and MEK7 feature high structural[23] and functional[14b] homology, and selectively inhibiting one in the presence of the other is often difficult.[22,31a] We were surprised to not induce MEK4 inhibition at concentrations as high as 80 µM, prompting us to pursue further selectivity studies.

To better understand the selectivity profile of this class of inhibitors, **24** was subjected to a 97-kinase selectivity screen (Figure 5, ScanEDGE, DiscoverX/Eurofins; see Figure SI-9 for details).

Among the 97 off-target kinases surveyed, our lead compound only interacted significantly with EGFR and the EGFR(L858R) mutant at 1 μM (selectivity scores:[32] $S(35) = S(10) = 0.011$). Notably, **24** has no appreciable activity on MEK1/2, p38α/β, or JNK1/2/3, which are highly relevant kinases in our model for molecular pathophysiology in T-ALL.[8b,12-13,33] Remarkably, this compound also does not engage FLT3, a potential pitfall we had antic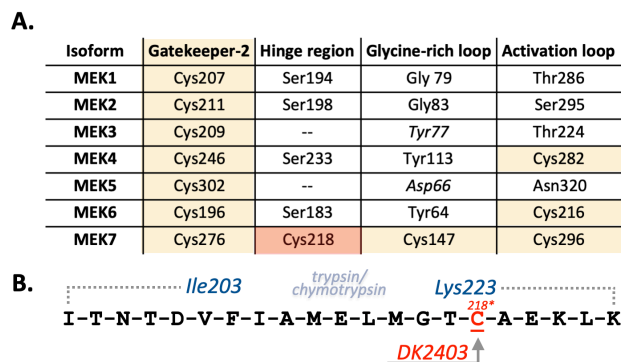ipated given the structural similarities between **24** and **4**, a reversible FLT3 inhibitor. Notably, MAP2K7 is not among the 90 wildtype kinases assayed and represented in Figure 5.

A.

Isoform	Gatekeeper-2	Hinge region	Glycine-rich loop	Activation loop
MEK1	Cys207	Ser194	Gly 79	Thr286
MEK2	Cys211	Ser198	Gly83	Ser295
MEK3	Cys209	--	Tyr77	Thr224
MEK4	Cys246	Ser233	Tyr113	Cys282
MEK5	Cys302	--	Asp66	Asn320
MEK6	Cys196	Ser183	Tyr64	Cys216
MEK7	Cys276	Cys218	Cys147	Cys296

B.

I-T-N-T-D-V-F-I-A-M-E-L-M-G-T-C-A-E-K-L-K

Figure 6. (A) Summary of active site cysteine residues among the MEK isoforms. Cys218, targeted by DK2403 (**24**), is highlighted in red. (B) Observed tandem mass spectrometry adduct confirming DK2403 covalently engages Cys218.

To study the action of DK2403 in living cells, the dose-response cytotoxicity of the compound was assessed in a variety of T-ALL cell lines. As shown in Figure 7A, **24** displayed marked cytotoxicity, surpassing the potency of **7** (Figure SI-3) and JNK-IN-8.[8b] To our knowledge, this represents the most cytotoxic MAP2K7 inhibitor towards T-ALL lines of interest with the exception of **1**[13a] and OTSSP167.[13b] The cytotoxicity of these compounds is likely multifactorial given their promiscuity,[34] and for **1**, low MAP2K7 potency ($IC_{50} = 1.3$ μM vs. 80 nM for MAP2K1 and 80 nM for TAK1).[18]
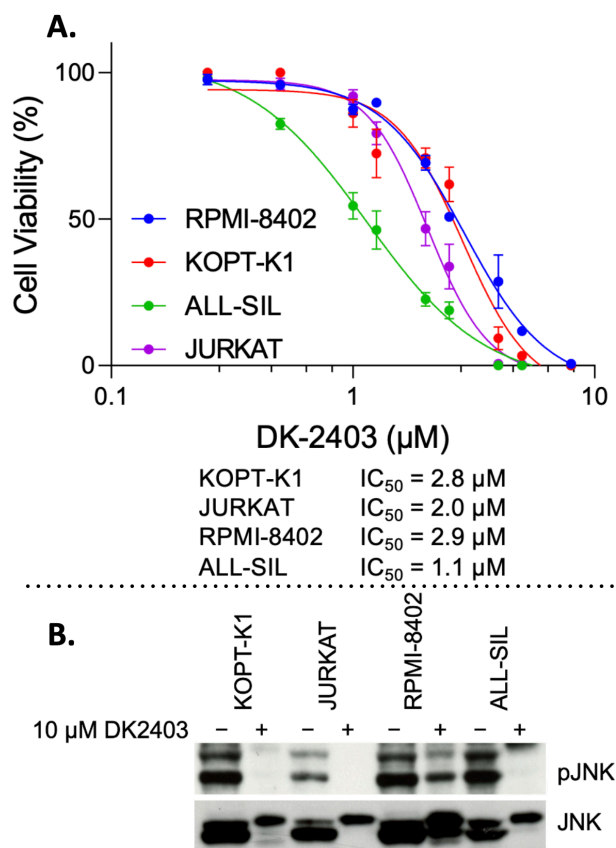

Figure 5. Off-target activity profile of **24**. Among 90 wildtype kinases surveyed, compound **24** only is appreciably bound by one kinase (EGFR, red dot) at 1 μM (not shown: mutant EGFR(L858R) also binds **24**).

To confirm the suspected covalent mechanism of DK2403 (**24**), full-length MAP2K7 N-terminal GST fusion protein (74 kDa) was incubated with MEK7 inhibitor **24** (2 equiv). After 12 h at 5 °C, the incubates were analyzed by LC-TOF MS. To our delight, MS analysis demonstrated covalent engagement of the inhibitor (see Figures SI-5 and SI-6). The experimental incubates were then digested with either trypsin/chymotrypsin combination or GluC. The former digest revealed covalent engagement of **24** with the intended Cys218 residue (Figures 6 and SI-7). Adducts involving other cysteine residues in the active site were not observed, although some labeling of solvent-exposed Cys341 was observed following GluC digestion (Figure SI-8). Selectivity of our most potent compound likely derives in part from targeting this unique cysteine residue in the active site, as only 11 human kinases bear a cysteine at the same relative position (Figure 6A).[26]

A.

KOPT-K1	IC_{50} = 2.8 μM
JURKAT	IC_{50} = 2.0 μM
RPMI-8402	IC_{50} = 2.9 μM
ALL-SIL	IC_{50} = 1.1 μM

B.

Figure 7. (A) Dose-response cytotoxicity of DK2403 (**24**) in T-ALL cell lines. (B) Western blot analysis demonstrating decreased phosphorylation of JNK in T-ALL cells following treatment with **24** (10 μM).

5

Further probing the cellular efficacy of our novel MAP2K7 inhibitor, we examined the effects of **24** on JNK phosphorylation. Treatment with **24** potently attenuated JNK phosphorylation at 10 μM (Figure 7B). Combined with our extremely clean selectivity profile $(S(35) = S(10) = 0.011)$, this finding strongly suggests that cytotoxicity is derived from attenuating the aberrant JNK phosphorylation described in these cell lines.[8b,12-13,33]

In conclusion, we have developed novel potent and selective MAP2K7 inhibitors that covalently engage the unique Cys218 residue within the active site. Our investigation commenced with a known FLT3 inhibitor with off-target activity against MAP2K7 previously identified by our group. Lead optimization activities were guided by an iterative cycle of computational modeling, synthesis, and *in vitro* evaluation. The rapid generation of chemical diversity was enabled by a streamlined one-pot process, much unlike the involved synthetic approaches required by compounds of similar selectivity profiles.[35] The preliminary selectivity studies described herein support that DK2403 (**24**) potently inhibits MAP2K7 without significant disruptions to the greater kinome, rendering it an excellent candidate for the study of MAP2K7 in the context of pediatric T-ALL.

ASSOCIATED CONTENT

Supporting Information

The Supporting Information is available free of charge on the ACS Publications website.

Additional *in vitro* results, additional cytotoxicity data, full selectivity data, PAMPA data, TOF-MS and MS-MS data, experimental details for *in vitro*, cellular, and MS experiments, modeling protocols, compound synthesis, and characterization.

AUTHOR INFORMATION

Corresponding Author

Karl A. Scheidt – Department of Chemistry, Northwestern University, Evanston, Illinois 60208, United States; Department of Pharmacology, Northwestern University, Chicago, Illinois 60611, United States; Chemistry of Life Processes Institute, Northwestern University, Evanston, Illinois 60208, United States. orcid.org/00000003-4856-3569; Email: scheidt@northwestern.edu

Authors

Dalton R. Kim – Department of Chemistry, Northwestern University, Evanston, Illinois 60208, United States

Meghan J. Orr – Department of Chemistry, Northwestern University, Evanston, Illinois 60208, United States

Ada J. Kwong – Department of Chemistry, Northwestern University, Evanston, Illinois 60208, United States

Kristine K. Deibler – Department of Chemistry, Northwestern University, Evanston, Illinois 60208, United States

Hasan H. Munshi – Department of Chemistry, Northwestern University, Evanston, Illinois 60208, United States

Cory Seth Bridges – Department of Pathology & Immunology, Baylor College of Medicine, Houston, Texas 77030, United States

Taylor Jie Chen – Department of Pathology & Immunology, Baylor College of Medicine, Houston, Texas 77030, United States

Xiaoyu Zhang – Department of Chemistry, Northwestern University, Evanston, Illinois 60208, United States; Chemistry of Life Processes Institute, Northwestern University, Evanston, Illinois 60208, United States.

H. Daniel Lacorazza – Department of Pathology & Immunology, Baylor College of Medicine, Houston, Texas 77030, United States

Author Contributions

D.R.K., K.K.D., and K.A.S. conceived the project. D.R.K. and K.A.S. directed the project. D.R.K. and H.H.M. conducted all organic synthesis and characterization. M.J.O. conducted all docking studies and computational modeling. D.R.K., M.J.O., and A.J.K completed all *in vitro* assays. C.S.B. and T.J.C. completed all cellular assays with direction from H.D.L. D.R.K. completed whole-protein LC/MS-TOF experiments. X.Z. completed protein digestion and MS-MS experiments. The manuscript was written through contributions of all authors. All authors have given approval to the final version of the manuscript.

Notes

The authors declare no competing financial interests.

ABBREVIATIONS

ALL, acute lymphoblastic leukemia; KLF4, Krüppel-like factor 4; MAP2K7, mitogen-activated protein kinase kinase 7; MEK7, MAPK/Erk kinase 7; JNK, *c*-Jun *N*-terminal kinase; 5Z7O, 5Z-7-oxozeaenol; TAK1, transforming growth factor-β (TGF-β)-activated kinase 1; EGFR, epidermal growth factor receptor; FLT3, FMS-like-tyrosine kinase 3; GST, glutathione *S*-transferase.

REFERENCES

(1) Hunger, S. P.; Mullighan, C. G. *N. Engl. J. Med.* **2015**, *373*, 1541-1552.
(2) Pui, C.-H.; Robison, L. L.; Look, A. T. *Lancet* **2008**, *371*, 1030-1043.

(3) (a) Pui, C.-H.; Evans, W. E. *N. Engl. J. Med.* **2006**, *354*, 166-178; (b) Pui, C. H.; Carroll, W. L.; Meshinchi, S.; Arceci, R. J. *J. Clin. Oncol.* **2011**, *29*, 551-565.

(4) (a) Linabery, A. M.; Ross, J. A. *Cancer* **2008**, *112*, 416-432; (b) Linabery, A. M.; Ross, J. A. *Cancer* **2008**, *113*, 2575-2596.

(5) Ko, R. H.; Ji, L.; Barnette, P.; Bostrom, B.; Hutchinson, R.; Raetz, E.; Seibel, N. L.; Twist, C. J.; Eckroth, E.; Sposto, R.; Gaynon, P. S.; Loh, M. L. *J. Clin. Oncol.* **2010**, *28*, 648-654.

(6) Oeffinger, K. C.; Mertens, A. C.; Sklar, C. A.; Kawashima, T.; Hudson, M. M.; Meadows, A. T.; Friedman, D. L.; Marina, N.; Hobbie, W.; Kadan-Lottick, N. S.; Schwartz, C. L.; Leisenring, W.; Robison, L. L. *N. Engl. J. Med.* **2006**, *355*, 1572-1582.

(7) Pinkel, D. *JAMA* **1971**, *216*, 648-652.

(8) (a) Kantarjian, H.; Thomas, D.; Wayne, A. S.; O'Brien, S. *J. Clin. Oncol.* **2012**, *30*, 3876-3883; (b) Shen, Y.; Park, C. S.; Suppipat, K.; Mistretta, T. A.; Puppi, M.; Horton, T. M.; Rabin, K.; Gray, N. S.; Meijerink, J. P. P.; Lacorazza, H. D. *Leukemia* **2017**, *31*, 1314-1324.

(9) Shields, J. M.; Christy, R. J.; Yang, V. W. *J. Biol. Chem.* **1996**, *271*, 20009-20017.

(10) (a) Black, A. R.; Black, J. D.; Azizkhan-Clifford, J. *J. Cell. Physiol.* **2001**, *188*, 143-160; (b) Rowland, B. D.; Bernards, R.; Peeper, D. S. *Nat. Cell Biol.* **2005**, *7*, 1074-1082.

(11) (a) Kang, H.; Chen, I.-M.; Wilson, C. S.; Bedrick, E. J.; Harvey, R. C.; Atlas, S. R.; Devidas, M.; Mullighan, C. G.; Wang, X.; Murphy, M.; Ar, K.; Wharton, W.; Borowitz, M. J.; Bowman, W. P.; Bhojwani, D.; Carroll, W. L.; Camitta, B. M.; Reaman, G. H.; Smith, M. A.; Downing, J. R.; Hunger, S. P.; Willman, C. L. *Blood* **2010**, *115*, 1394-1405; (b) Malik, D.; Kaul, D.; Chauhan, N.; Marwaha, R. K. *Mol. Cancer* **2014**, *13*, 175-175.

(12) Lacorazza, H. D. *Oncotarget* **2017**, *8*, 73366-73367.

(13) (a) Chen, T. J.; Du, W.; Junco, J. J.; Bridges, C. S.; Shen, Y.; Puppi, M.; Rabin, K. R.; Lacorazza, H. D. *Oncotarget* **2021**, *12*, 1787-1801; (b) Bridges, C. S.; Chen, T. J.; Puppi, M.; Rabin, K. R.; Lacorazza, H. D. *Blood Advances* **2022**, bloodadvances.2022008548.

(14) Platanias, L. C. *Blood* **2003**, *101*, 4667.

(15) Van Meter, M.; Simon, M.; Tombline, G.; May, A.; Morello, T. D.; Hubbard, B. P.; Bredbenner, K.; Park, R.; Sinclair, D. A.; Bohr, V. A.; Gorbunova, V.; Seluanov, A. *Cell Rep.* **2016**, *16*, 2641-2650.

(16) Calses, P. C.; Dhillon, K. K.; Tucker, N.; Chi, Y.; Huang, J. W.; Kawasumi, M.; Nghiem, P.; Wang, Y.; Clurman, B. E.; Jacquemont, C.; Gafken, P. R.; Sugasawa, K.; Saijo, M.; Taniguchi, T. *Cell Rep.* **2017**, *19*, 162-174.

(17) Kwong, A. J.; Scheidt, K. A. *Bioorganic Med. Chem. Lett.* **2020**, *30*, 127203.

(18) Sogabe, Y.; Matsumoto, T.; Hashimoto, T.; Kirii, Y.; Sawa, M.; Kinoshita, T. *Bioorganic Med. Chem. Lett.* **2015**, *25*, 593-596.

(19) Wu, J.; Powell, F.; Larsen, N. A.; Lai, Z.; Byth, K. F.; Read, J.; Gu, R. F.; Roth, M.; Toader, D.; Saeh, J. C.; Chen, H. *ACS Chem. Biol.* **2013**, *8*, 643-650.

(20) Shraga, A.; Olshvang, E.; Davidzohn, N.; Khoshkenar, P.; Germain, N.; Shurrush, K.; Carvalho, S.; Avram, L.; Albeck, S.; Unger, T.; Lefker, B.; Subramanyam, C.; Hudkins, R. L.; Mitchell, A.; Shulman, Z.; Kinoshita, T.; London, N. *Cell Chem. Biol.* **2019**, *26*, 98-108.e105.

(21) Wolle, P.; Hardick, J.; Cronin, S. J. F.; Engel, J.; Baumann, M.; Lategahn, J.; Penninger, J. M.; Rauh, D. *J. Med. Chem.* **2019**, *62*, 2843-2848.

(22) Jiang, J.; Jiang, B.; He, Z.; Ficarro, S. B.; Che, J.; Marto, J. A.; Gao, Y.; Zhang, T.; Gray, N. S. *Cell Chem. Biol.* **2020**, *27*, 1553-1560.e1558.

(23) Deibler, K. K.; Mishra, R. K.; Clutter, M. R.; Antanasijevic, A.; Bergan, R.; Caffrey, M.; Scheidt, K. A. *ACS Chem. Biol.* **2017**, *12*, 1245-1256.

(24) Worzella, T.; Butzler, M.; Hennek, J.; Hanson, S.; Simdon, L.; Goueli, S.; Cowan, C.; Zegzouti, H. *SLAS Technol.* **2017**, *22*, 153-162.

(25) (a) Shieh, W.-C.; McKenna, J.; Sclafani, J. A.; Xue, S.; Girgis, M.; Vivelo, J.; Radetich, B.; Prasad, K. *Org. Process Res. Dev.* **2008**, *12*, 1146-1155; (b) Weisberg, E.; Roesel, J.; Bold, G.; Furet, P.; Jiang, J.; Cools, J.; Wright, R. D.; Nelson, E.; Barrett, R.; Ray, A. *Blood* **2008**, *112*, 5161-5170; (c) Akeno-Stuart, N.; Croyle, M.; Knauf, J. A.; Malaguarnera, R.; Vitagliano, D.; Santoro, M.; Stephan, C.; Grosios, K.; Wartmann, M.; Cozens, R.; Caravatti, G.; Fabbro, D.; Lane, H. A.; Fagin, J. A. *Cancer Res.* **2007**, *67*, 6956-6964.

(26) Liu, Q.; Sabnis, Y.; Zhao, Z.; Zhang, T.; Buhrlage, Sara J.; Jones, Lyn H.; Gray, Nathanael S. *Chem. Biol.* **2013**, *20*, 146-159.

(27) Gehringer, M.; Laufer, S. A. *J. Med. Chem.* **2019**, *62*, 5673-5724.

(28) Flanagan, M. E.; Abramite, J. A.; Anderson, D. P.; Aulabaugh, A.; Dahal, U. P.; Gilbert, A. M.; Li, C.; Montgomery, J.; Oppenheimer, S. R.; Ryder, T.; Schuff, B. P.; Uccello, D. P.; Walker, G. S.; Wu, Y.; Brown, M. F.; Chen, J. M.; Hayward, M. M.; Noe, M. C.; Obach, R. S.; Philippe, L.; Shanmugasundaram, V.; Shapiro, M. J.; Starr, J.; Stroh, J.; Che, Y. *J. Med. Chem.* **2014**, *57*, 10072-10079.

(29) Lu, W.; Kostic, M.; Zhang, T.; Che, J.; Patricelli, M. P.; Jones, L. H.; Chouchani, E. T.; Gray, N. S. *RSC Chem. Biol.* **2021**, *2*, 354-367.

(30) (a) Douangamath, A.; Fearon, D.; Gehrtz, P.; Krojer, T.; Lukacik, P.; Owen, C. D.; Resnick, E.; Strain-Damerell, C.; Aimon, A.; Ábrányi-Balogh, P.; Brandão-Neto, J.; Carbery, A.; Davison, G.; Dias, A.; Downes, T. D.; Dunnett, L.; Fairhead, M.; Firth, J. D.; Jones, S. P.; Keeley, A.; Keserü, G. M.; Klein, H. F.; Martin, M. P.; Noble, M. E. M.; O'Brien, P.; Powell, A.; Reddi, R. N.; Skyner, R.; Snee, M.; Waring, M. J.; Wild, C.; London, N.; von Delft, F.; Walsh, M. A. *Nat. Commun.* **2020**, *11*, 5047; (b) Resnick, E.; Bradley, A.; Gan, J.; Douangamath, A.; Krojer, T.; Sethi, R.; Geurink, P. P.; Aimon, A.; Amitai, G.; Bellini, D.; Bennett, J.; Fairhead, M.; Fedorov, O.; Gabizon, R.; Gan, J.; Guo, J.; Plotnikov, A.; Reznik, N.; Ruda, G. F.; Díaz-Sáez, L.; Straub, V. M.; Szommer, T.; Velupillai, S.; Zaidman, D.; Zhang, Y.; Coker, A. R.; Dowson, C. G.; Barr, H. M.; Wang, C.; Huber, K. V. M.; Brennan, P. E.; Ovaa, H.; von Delft, F.; London, N. *J. Am. Chem. Soc.* **2019**, *141*, 8951-8968.

(31) (a) Kwong, A. J.; Pham, T. N. D.; Oelschlager, H. E.; Munshi, H. G.; Scheidt, K. A. *ACS Med. Chem. Lett.* **2021**, *12*, 1559-1567; (b) Deibler, K. K.; Schiltz, G. E.; Clutter, M. R.; Mishra, R. K.; Vagadia, P. P.; O'Connor, M.; George, M. D.; Gordon, R.; Fowler, G.; Bergan, R.; Scheidt, K. A. *ChemMedChem* **2019**, *14*, 615-620.

(32) Karaman, M. W.; Herrgard, S.; Treiber, D. K.; Gallant, P.; Atteridge, C. E.; Campbell, B. T.; Chan, K. W.; Ciceri, P.; Davis, M. I.; Edeen, P. T.; Faraoni, R.; Floyd, M.; Hunt, J. P.; Lockhart, D. J.; Milanov, Z. V.; Morrison, M. J.; Pallares, G.; Patel, H. K.; Pritchard, S.; Wodicka, L. M.; Zarrinkar, P. P. *Nat. Biotechnol.* **2008**, *26*, 127-132.

(33) Shen, Y.; Chen, T. J.; Lacorazza, H. D. *Exp. Hematol.* **2017**, *53*, 16-25.

(34) (a) Ellestad, G. A. *Chirality* **2019**, *31*, 110-117; (b) Klaeger, S.; Heinzlmeir, S.; Wilhelm, M.; Polzer, H.; Vick, B.; Koenig, P.-A.; Reinecke, M.; Ruprecht, B.; Petzoldt, S.; Meng, C.; Zecha, J.; Reiter, K.; Qiao, H.; Helm, D.; Koch, H.; Schoof, M.; Canevari, G.; Casale, E.; Depaolini Stefania, R.; Feuchtinger, A.; Wu, Z.; Schmidt, T.; Rueckert, L.; Becker, W.; Huenges, J.; Garz, A.-K.; Gohlke, B.-O.; Zolg Daniel, P.; Kayser, G.; Vooder, T.; Preissner, R.; Hahne, H.; Tõnisson, N.; Kramer, K.; Götze, K.; Bassermann, F.; Schlegl, J.; Ehrlich, H.-C.; Aiche, S.; Walch, A.; Greif Philipp, A.; Schneider, S.; Felder Eduard, R.; Ruland, J.; Médard, G.; Jeremias, I.; Spiekermann, K.; Kuster, B. *Science* **2017**, *358*, 6367, eaan4368.

(35) (a) Chandregowda, V.; Venkateswara Rao, G.; Chandrasekara Reddy, G. *Org. Process Res. Dev.* **2007**, *11*, 813-816; (b) Kompella, A.; Adibhatla, B. R. K.; Muddasani, P. R.; Rachakonda, S.; Gampa, V. K.; Dubey, P. K. *Org. Process Res. Dev.* **2012**, *16*, 1794-1804.

I-T-N-T-D-V-F-I-A-M-E-L-M-G-T-C-A-E-K-L-K

Highly selective, covalent
α-chloroacetamide inhibitor
(app. IC$_{50}$ = 10 nM)

DK2403